Conditional simulations of extremal Gaussian processes

Clément Dombry† Mathieu Ribatet‡

† Laboratoire de Mathématiques et Application, Université de Poitiers, Téléport 2, BP 30179, F–86962 Futuroscope–Chasseneuil cedex, France
clement.dombry@math.univ-poitiers.fr

‡ Department of Mathematics, Université Montpellier 2, 4 place Eugène Bataillon, 34095 cedex 2 Montpellier, France
mathieu.ribatet@math.univ-montp2.fr

Abstract

Recently the regular conditional distributions of max-infinitely divisible processes were derived by Dombry and Éyi-Minko [2011] and although these conditional distributions have complicated closed forms, Dombry et al. [2011] introduce an algorithm to get conditional realizations of Brown–Resnick processes. In this paper we derive the regular conditional distributions of the max-stable process introduced by Schlather [2002] and adapt the framework of Dombry et al. [2011] to this specific process. We test the methods on simulated data and give an application to extreme temperatures in Switzerland. Results show that the proposed sampling scheme provide accurate conditional simulations and can handle real-sized problems.

Some key words: Conditional simulation, Max-stable process, Regular conditional distribution, Schlather process, Spatial extreme, Temperature.

1 Introduction

Max-stable processes play a major role in the statistical modelling of spatial extremes since they arise as an extension of the extreme value theory to the infinite dimensional case, i.e., extremes of stochastic processes. Motivated by the need of suitable models for the areal modelling extremes of environmental processes such as heat waves or rainfall, the last decade has seen many advances to develop a geostatistics of extremes. For instance Cooley et al. [2006] and Naveau et al. [2009] develop variogram like tools to assess the spatial dependence of extremes while Padoan et al. [2010] propose an inferential procedure based on the maximum pairwise likelihood estimator to fit max-stable processes to extreme spatial data sets. A broad overview of the different approaches available for the statistical modelling of spatial extremes is given by Davison et al. [2011].

Although conditional simulations of Gaussian based stochastic processes are known for a long time [Chilès and Delfiner, 1999], conditional simulation of max-stable processes is a long standing problem and a first attempt dates back to the works of Davis and Resnick [1993, 1989]. Recently this problem enjoyed renewed interest with the pioneer work of Wang and Stoev [2011] who give an efficient procedure to get conditional simulations of max-stable processes with discrete spectral measures. Dombry and Éyi-Minko [2011] derive the (regular) conditional distribution of max-infinitely divisible processes and an algorithm to get conditional realizations of Brown–Resnick processes is given by Dombry et al. [2011].

Although theoretical expressions exist for the general framework of max-infinitely divisible processes, there are only few models where these expressions are tractable and where efficient simulation algorithms are possible. The aim of this paper is to get conditional simulations for the extremal Gaussian process also known as the Schlather process [Schlather, 2002]

$$Z(x) = \sqrt{2\pi} \max_{i \geq 1} \zeta_i \max\{0, \varepsilon_i(x)\}, \qquad x \in \mathbb{R}^d, \tag{1}$$

where $\{\zeta_i\}_{i \geq 1}$ are the points of a Poisson process on $(0, \infty)$ with intensity measure $\mathrm{d}\Lambda(\zeta) = \zeta^{-2}\mathrm{d}\zeta$ and ε_i are independent copies of a standard Gaussian process with correlation function ρ. The processes ε_i are

assumed to be independent of the points $\{\zeta_i\}_{i\geq 1}$. It is well known that the process (1) is a max-stable process with unit Fréchet margins whose finite dimensional distribution functions are [Schlather, 2002]

$$\Pr[Z(x_1) \leq z_1, \ldots, Z(x_k) \leq z_k] = \exp\left\{-\mathbb{E}\left[\sqrt{2\pi}\max_{j=1,\ldots,k}\frac{\max\{0,\varepsilon(x_j)\}}{z_j}\right]\right\},$$

for all $k \in \mathbb{N}$, $x_1, \ldots, x_k \in \mathbb{R}^d$, $z_1, \ldots, z_k > 0$, and that its extremal coefficient function is

$$\theta(h) = 1 + \sqrt{\frac{1-\rho(h)}{2}}, \qquad h \in \mathbb{R}^d.$$

An important property of the Schlather process is that it cannot reach independence at long distances since $\theta(h) \to 1 + \sqrt{1/2}$ as $\|h\| \to \infty$. Recall that independence is reached when $\theta(h) = 2$ and that when $\theta(h) \to 2$ as $\|h\| \to \infty$ the max-stable process is mixing [Kabluchko and Schlather, 2010].

Given a study region $\mathcal{X} \subset \mathbb{R}^d$, our goal is to sample from $Z \mid \{Z(x_1) = z_1, \ldots, Z(x_k) = z_k\}$ for some $(x_1, \ldots, x_k) \in \mathcal{X}^k$, $k \in \mathbb{N}$, and $(z_1, \ldots, z_k) \in (0, \infty)^k$. In Section 2 we derive the (regular) conditional distribution of the Schlather process and recall the sampling scheme introduced by Dombry et al. [2011]. Section 3 analyzes the performance of this algorithm on simulated data. The paper ends with an application on extreme temperatures in Switzerland followed by a brief discussion.

2 Conditional simulation of Schlather processes

This section aims at deriving the regular conditional distribution of Schlather processes. For our purposes, instead of working with the spectral characterization (1), it is more convenient to use the following representation

$$Z(x) = \sqrt{2\pi}\max_{i\geq 1}\zeta_i\varepsilon_i(x), \tag{2}$$

where $\{\zeta_i\}_{i\geq 1}$ and ε_i are defined as in (1). These two spectral characterizations are equivalent since Z corresponds to pointwise maxima over an infinite number of random functions and consequently the negative parts of the Gaussian processes ε_i have no contribution. More formally for $x \in \mathcal{X}$, we have

$$\Pr[Z(x) \leq 0] = \exp\left\{-\int_0^\infty \mathbb{E}\left[1_{\{\sqrt{2\pi}\zeta\varepsilon(x)>0\}}\right]\zeta^{-2}\mathrm{d}\zeta\right\} = \exp\left\{-\int_0^\infty \frac{1}{2}1_{\{\zeta>0\}}\zeta^{-2}\mathrm{d}\zeta\right\} = 0,$$

and for $k \in \mathbb{N}$, $(x_1, \ldots, x_k) \in \mathcal{X}^k$ and $z_1, \ldots, z_k > 0$

$$\begin{aligned}\Pr[Z(x_1) \leq z_1, \ldots, Z(x_k) \leq z_k] &= \exp\left\{-\int_0^\infty \mathbb{E}\left[1_{\{\exists j\in\{1,\ldots,k\},\ \sqrt{2\pi}\zeta\varepsilon(x_j)>z_j\}}\right]\zeta^{-2}\mathrm{d}\zeta\right\}\\ &= \exp\left\{-\sqrt{2\pi}\mathbb{E}\left[\max_{j=1,\ldots,k}\frac{\max\{0,\varepsilon(x_j)\}}{z_j}\right]\right\}.\end{aligned}$$

This shows that the processes (1) and (2) have the same finite dimensional distributions.

Let $\mathbb{C}_0$ be the space of real valued continuous functions on $\mathcal{X} \subset \mathbb{R}^d$ and $\Phi = \{\varphi_i\}_{i\geq 1}$ a Poisson point process on $\mathbb{C}_0$ such that

$$\varphi_i(x) = \sqrt{2\pi}\zeta_i\varepsilon_i(x), \qquad i = 1, 2, \ldots,$$

with $\{\zeta_i\}_{i\geq 1}$ and ε_i are defined as in (1). To shorten the notations we write $f(\mathbf{x}) = \{f(x_1), \ldots, f(x_k)\}$ for all (random) function $f\colon \mathcal{X} \to \mathbb{R}$ and $\mathbf{x} = (x_1, \ldots, x_k) \in \mathcal{X}^k$.

For $\mathbf{x} \in \mathcal{X}^k$, the Poisson point process $\{\varphi_i(\mathbf{x})\}_{i\geq 1}$ defined on $\mathbb{R}^k$ has intensity measure

$$\Lambda_{\mathbf{x}}(A) = \int_0^\infty \Pr[\sqrt{2\pi}\zeta\varepsilon(\mathbf{x}) \in A]\zeta^{-2}\mathrm{d}\zeta, \qquad A \subset \mathbb{R}^k \text{ Borel set},$$

where $\varepsilon(\mathbf{x})$ is a centered multivariate normal random vector with covariance matrix $\Sigma_{\mathbf{x}} = \{\rho(x_i - x_j)\}_{i,j}$, $i, j = 1, \ldots, k$. Provided the covariance matrix $\Sigma_{\mathbf{x}}$ is positive definite, it can be shown—see Appendix A, that the intensity measure $\Lambda_{\mathbf{x}}$ is absolutely continuous with respect to the Lebesgue measure and that the density of $\Lambda_{\mathbf{x}}$ is

$$\lambda_{\mathbf{x}}(\mathbf{z}) = \pi^{-(k-1)/2}|\Sigma_{\mathbf{x}}|^{-1/2}a_{\mathbf{x}}(\mathbf{z})^{-(k+1)/2}\Gamma\left(\frac{k+1}{2}\right), \qquad \mathbf{z} \in \mathbb{R}^k,$$

where $a_{\mathbf{x}}(\mathbf{z}) = \mathbf{z}^T \Sigma_{\mathbf{x}}^{-1} \mathbf{z}$.

The explicit expression of the density $\lambda_{\mathbf{x}}(\mathbf{z})$ is the starting point of the methodology developed in Dombry et al. [2011] where it is shown that the quotient

$$\lambda_{\mathbf{s}|\mathbf{x},\mathbf{z}}(\mathbf{u}) = \frac{\lambda_{(\mathbf{s},\mathbf{x})}(\mathbf{u},\mathbf{z})}{\lambda_{\mathbf{x}}(\mathbf{z})}, \qquad \mathbf{u} \in \mathbb{R}^m,$$

characterizes the density of the extremal functions, i.e., the atoms of Φ that reach (at least) one hitting bound $Z(x_i) = z_i$ for some $i \in \{1, \dots, k\}$. Consequently to be able to draw conditional simulations from the process (1), the distributions of the extremal functions have to be identified.

Proposition 1. *For $(\mathbf{s}, \mathbf{x}) \in \mathcal{X}^{m+k}$, $\mathbf{z} \in \mathbb{R}^k$ and provided that the covariance matrix $\Sigma_{(\mathbf{s},\mathbf{x})}$ of the random vector $\varepsilon\{(\mathbf{s}, \mathbf{x})\}$ is positive definite, the function $\lambda_{\mathbf{s}|\mathbf{x},\mathbf{z}}(\mathbf{u})$, $\mathbf{u} \in \mathbb{R}^m$, corresponds to the density of a multivariate Student distribution with $k+1$ degrees of freedom, location parameter*

$$\mu = \Sigma_{\mathbf{s}:\mathbf{x}} \Sigma_{\mathbf{x}}^{-1} \mathbf{z},$$

and scale matrix

$$\tilde{\Sigma} = \frac{a_{\mathbf{x}}(\mathbf{z})}{k+1} \left(\Sigma_{\mathbf{s}} - \Sigma_{\mathbf{s}:\mathbf{x}} \Sigma_{\mathbf{x}}^{-1} \Sigma_{\mathbf{x}:\mathbf{s}} \right), \qquad \Sigma_{(\mathbf{s},\mathbf{x})} = \begin{bmatrix} \Sigma_{\mathbf{s}} & \Sigma_{\mathbf{s}:\mathbf{x}} \\ \Sigma_{\mathbf{x}:\mathbf{s}} & \Sigma_{\mathbf{x}} \end{bmatrix}.$$

Proof. For all $\mathbf{u} \in \mathbb{R}^m$ we have

$$\lambda_{\mathbf{s}|\mathbf{x},\mathbf{z}}(\mathbf{u}) = \pi^{-m/2} \frac{|\Sigma_{(\mathbf{s},\mathbf{x})}|^{-1/2}}{|\Sigma_{\mathbf{x}}|^{-1/2}} \left\{ \frac{a_{(\mathbf{s},\mathbf{x})}(\mathbf{u},\mathbf{z})}{a_{\mathbf{x}}(\mathbf{z})} \right\}^{-(m+k+1)/2} a_{\mathbf{x}}(\mathbf{z})^{-m/2} \frac{\Gamma\left(\frac{m+k+1}{2}\right)}{\Gamma\left(\frac{k+1}{2}\right)}.$$

We start by focusing on the ratio $a_{(\mathbf{s},\mathbf{x})}(\mathbf{u},\mathbf{z})/a_{\mathbf{x}}(\mathbf{z})$. Since

$$\begin{bmatrix} \Sigma_{\mathbf{s}} & \Sigma_{\mathbf{s}:\mathbf{x}} \\ \Sigma_{\mathbf{x}:\mathbf{s}} & \Sigma_{\mathbf{x}} \end{bmatrix}^{-1} = \begin{bmatrix} (\Sigma_{\mathbf{s}} - \Sigma_{\mathbf{s}:\mathbf{x}} \Sigma_{\mathbf{x}}^{-1} \Sigma_{\mathbf{x}:\mathbf{s}})^{-1} & -(\Sigma_{\mathbf{s}} - \Sigma_{\mathbf{s}:\mathbf{x}} \Sigma_{\mathbf{x}}^{-1} \Sigma_{\mathbf{x}:\mathbf{s}})^{-1} \Sigma_{\mathbf{s}:\mathbf{x}} \Sigma_{\mathbf{x}}^{-1} \\ -\Sigma_{\mathbf{x}}^{-1} \Sigma_{\mathbf{x}:\mathbf{s}} (\Sigma_{\mathbf{s}} - \Sigma_{\mathbf{s}:\mathbf{x}} \Sigma_{\mathbf{x}}^{-1} \Sigma_{\mathbf{x}:\mathbf{s}})^{-1} & \Sigma_{\mathbf{x}}^{-1} + \Sigma_{\mathbf{x}}^{-1} \Sigma_{\mathbf{x}:\mathbf{s}} (\Sigma_{\mathbf{s}} - \Sigma_{\mathbf{s}:\mathbf{x}} \Sigma_{\mathbf{x}}^{-1} \Sigma_{\mathbf{x}:\mathbf{s}})^{-1} \Sigma_{\mathbf{s}:\mathbf{x}} \Sigma_{\mathbf{x}}^{-1} \end{bmatrix},$$

straightforward algebra shows that

$$\frac{a_{(\mathbf{s},\mathbf{x})}(\mathbf{u},\mathbf{z})}{a_{\mathbf{x}}(\mathbf{z})} = 1 + \frac{(\mathbf{u}-\mu)^T \tilde{\Sigma}^{-1} (\mathbf{u}-\mu)}{k+1}, \qquad \mu = \Sigma_{\mathbf{s}:\mathbf{x}} \Sigma_{\mathbf{x}}^{-1} \mathbf{z}, \qquad \tilde{\Sigma} = \frac{a_{\mathbf{x}}(\mathbf{z})}{k+1} \left(\Sigma_{\mathbf{s}} - \Sigma_{\mathbf{s}:\mathbf{x}} \Sigma_{\mathbf{x}}^{-1} \Sigma_{\mathbf{x}:\mathbf{s}} \right).$$

We now try to simplify the ratio $|\Sigma_{(\mathbf{s},\mathbf{x})}|/|\Sigma_{\mathbf{x}}|$. Using the fact that

$$\Sigma_{(\mathbf{s},\mathbf{x})} = \begin{bmatrix} \Sigma_{\mathbf{s}} & \Sigma_{\mathbf{s}:\mathbf{x}} \\ \Sigma_{\mathbf{x}:\mathbf{s}} & \Sigma_{\mathbf{x}} \end{bmatrix} = \begin{bmatrix} \mathrm{Id} & \Sigma_{\mathbf{s}:\mathbf{x}} \\ \mathbf{0} & \Sigma_{\mathbf{x}} \end{bmatrix} \begin{bmatrix} \Sigma_{\mathbf{s}} - \Sigma_{\mathbf{s}:\mathbf{x}} \Sigma_{\mathbf{x}}^{-1} \Sigma_{\mathbf{x}:\mathbf{s}} & \mathbf{0} \\ \Sigma_{\mathbf{x}}^{-1} \Sigma_{\mathbf{x}:\mathbf{s}} & \mathrm{Id} \end{bmatrix},$$

where Id is the identity matrix, $\mathbf{0}$ is a matrix with zero entries, combined with some more algebra yields

$$\frac{|\Sigma_{(\mathbf{s},\mathbf{x})}|}{|\Sigma_{\mathbf{x}}|} = |\Sigma_{\mathbf{s}} - \Sigma_{\mathbf{s}:\mathbf{x}} \Sigma_{\mathbf{x}}^{-1} \Sigma_{\mathbf{x}:\mathbf{s}}| = \left\{ \frac{k+1}{a_{\mathbf{x}}(\mathbf{z})} \right\}^m |\tilde{\Sigma}|.$$

Using the two previous results it is easily found that

$$\lambda_{\mathbf{s}|\mathbf{x},\mathbf{z}}(\mathbf{u}) = \pi^{-m/2} (k+1)^{-m/2} |\tilde{\Sigma}|^{-1/2} \left\{ 1 + \frac{(\mathbf{u}-\mu)^T \tilde{\Sigma}^{-1} (\mathbf{u}-\mu)}{k+1} \right\}^{-(m+k+1)/2} \frac{\Gamma\left(\frac{m+k+1}{2}\right)}{\Gamma\left(\frac{k+1}{2}\right)},$$

which corresponds to the density of a multivariate Student distribution with the expected parameters. □

At first sight it seems intriguing that the extremal functions involve a multivariate Student distribution. However this result is not as surprising as it might be at first glance. Indeed consider the following simple max-stable process

$$\tilde{Z}(x) = c\sqrt{2\pi} \max_{i \geq 1} \zeta_i X_i^{1/2} \max\{0, \varepsilon_i(x)\}, \qquad c^{-1} = \mathbb{E}\left[X^{1/2} \right], \qquad \nu > 1,$$

where the normalizing constant c appears to ensure unit Fréchet margins, $\{\zeta_i\}_{i\geq 1}$ are the points of a Poisson process on $(0,\infty)$ with intensity $\mathrm{d}\Lambda(\zeta)=\zeta^{-2}\mathrm{d}\zeta$, X_i are independent copies of a random variable X such that ν/X follows a χ^2 distribution with ν degrees of freedom and ε_i are independent replicates of a standard Gaussian process as in (1). All these random objects are assumed to be mutually independent. It is easily shown that

$$\begin{aligned}\Pr[\tilde{Z}(x_1)\leq z_1,\ldots,\tilde{Z}(x_k)\leq z_k] &= \exp\left\{-\mathbb{E}\left[c\sqrt{2\pi}\max_{j=1,\ldots,k} X^{1/2}\frac{\max\{0,\varepsilon(x_j)\}}{z_j}\right]\right\}\\ &= \exp\left\{-c\sqrt{2\pi}\mathbb{E}\left[X^{1/2}\right]\mathbb{E}\left[\max_{j=1,\ldots,k}\frac{\max\{0,\varepsilon(x_j)\}}{z_j}\right]\right\}\\ &= \exp\left\{-\sqrt{2\pi}\mathbb{E}\left[\max_{j=1,\ldots,k}\frac{\max\{0,\varepsilon(x_j)\}}{z_j}\right]\right\}\\ &= \Pr[Z(x_1)\leq z_1,\ldots,Z(x_k)\leq z_k],\end{aligned}$$

and the original Schlather process defined through standard Gaussian processes by Schlather [2002] has an equivalent construction based on Student processes.

A similar result as Proposition 1 holds for the Brown-Resnick process where $\lambda_{\mathbf{s}|\mathbf{x},\mathbf{z}}(\mathbf{u})$ corresponds to the density of a multivariate log-normal distribution instead of a multivariate Student distribution. In spite of this difference, the method for conditional simulation of Brown-Resnick processes proposed by Dombry et al. [2011] can be adapted straightforwardly to obtain conditional simulations of a Schlather process. For consistency we briefly recall the procedure:

Step 1 Draw a random partition θ of the set $\{x_1,\ldots,x_k\}$ from the following distribution

$$\Pr[\theta=\tau\mid Z(\mathbf{x})=\mathbf{z}]\propto\prod_{j=1}^{|\tau|}\lambda_{\mathbf{x}_{\tau_j}}(\mathbf{z}_{\tau_j})\int_{\{\mathbf{u}_j<\mathbf{z}_{\tau_j^c}\}}\lambda_{\mathbf{x}_{\tau_j^c}|\mathbf{x}_{\tau_j},\mathbf{z}_{\tau_j}}(\mathbf{u}_j)\mathrm{d}\mathbf{u}_j,$$

where τ is a partition of $\{x_1,\ldots,x_k\}$, $|\tau|$ is the size of the partition, $\mathbf{v}_{\tau_j}=(v_i\colon i\in I_j)$ and $\mathbf{v}_{\tau_j^c}=(v_i\colon i\notin I_j)$ with $I_j=\{i\colon x_i\in\tau_j\}$ for all k-upple $\mathbf{v}$ living in $\mathcal{X}^k$ or $\mathbb{R}^k$;

Step 2 Given $\tau=(\tau_1,\ldots,\tau_\ell)$, draw ℓ independent extremal functions $\varphi_1^+,\ldots,\varphi_\ell^+$ whose finite dimensional distributions are

$$\Pr[\varphi_j^+(\mathbf{s})\in\mathrm{d}\mathbf{v}\mid Z(\mathbf{x})=\mathbf{z},\theta=\tau]\propto\left\{\int 1_{\{\mathbf{u}<\mathbf{z}_{\tau_j^c}\}}\lambda_{(\mathbf{s},\mathbf{x}_{\tau_j^c})|\mathbf{x}_{\tau_j},\mathbf{z}_{\tau_j}}(\mathbf{v},\mathbf{u})\mathrm{d}\mathbf{u}\right\}\mathrm{d}\mathbf{v},\qquad \mathbf{s}\in\mathcal{X}^m,\ m\in\mathbb{N},$$

where $1_{\{\cdot\}}$ is the indicator function and set $Z^+=\max(\varphi_1^+,\ldots,\varphi_\ell^+)$;

Step 3 Independently from the two previous steps, draw a Schlather process Z^- conditioned to the constraint $Z^-(\mathbf{x})\leq\mathbf{z}$ by thinning the Poisson point process Φ, i.e.,

$$Z^-=\max\{\varphi\in\Phi\colon\varphi(\mathbf{x})\leq\mathbf{z}\}.$$

Then, $\tilde{Z}=\max\{Z^+,Z^-\}$ follows the conditional distribution of Z given $Z(\mathbf{x})=\mathbf{z}$. We remind that the partition size ℓ denotes the number of extremal functions needed to satisfy the conditional event $Z(\mathbf{x})=\mathbf{z}$. The extremal function φ_j^+ associated to the component τ_j of τ satisfies the constraints $\varphi_j(x_i)=z_i$ if $x_i\in\tau_j$ and $\varphi_j(x_i)<z_i$ if $x_i\notin\tau_j$—see Theorem 1 in Dombry et al. [2011] for more details. Consequently in Step 2 a rejection algorithm has to be used to ensure that the sampled extremal functions meet these conditions.

For practical purposes, Step 1 is the more challenging since it amounts to sample from a discrete distribution whose state space corresponds to all possible partitions of the set $\{x_1,\ldots,x_k\}$. Since the number of possible partitions of a set with k elements corresponds to Bell numbers, it results in a combinatorial explosion even for a moderate number of conditioning locations. For instance when $k=10$ there are around 116000 possibilities. To bypass this computational burden, Dombry et al. [2011] propose the use of a Gibbs sampler in Step 1 and in the remainder of this paper, we will use their Gibbs sampler whenever k is too large, e.g., $k\geq 10$.

Table 1: *Spatial dependence structures of Schlather processes based on an isotropic powered exponential correlation function with scale parameter λ and shape parameter κ. The correlation function parameters are set to ensure that $\theta(100) = 1.5$.*

	Sample path properties		
	θ_1: Wiggly	θ_2: Smooth	θ_3: Very smooth
λ	208	144	128
κ	0.5	1	1.5

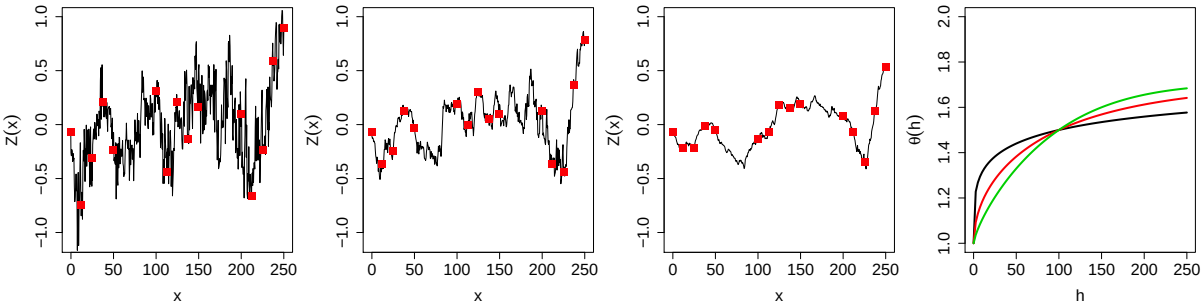

Figure 1: *Three (unconditional) realizations of a Schlather process with standard Gumbel margins and extremal coefficient functions θ_1, θ_2 and θ_3—from left to right. The squares correspond to the 15 conditioning values that will be used in the simulation study. The right panel shows the associated extremal coefficient functions where the black, red and green lines correspond respectively to θ_1, θ_2 and θ_3.*

3 Simulation Study

In this section we check whether our algorithm is able to produce realistic conditional simulations of Schlather processes. To this aim we consider an isotropic powered exponential correlation function

$$\rho(h) = \exp\left\{-\left(\frac{h}{\lambda}\right)^{\kappa}\right\}, \qquad h > 0, \quad \lambda > 0, \quad 0 < \kappa \leq 2,$$

and three different spatial dependence configurations as summarized in Table 1. Figure 2 shows one (unconditional) realization for each sample path configuration as well as the corresponding extremal coefficient functions. These realizations will serve as a basis for our conditioning events.

To check if our sampling procedure is accurate and given a single conditional event $Z(\mathbf{x}) = \mathbf{z}$, we generate 1000 conditional realizations of a Schlather process with standard Gumbel margins and extremal coefficient function θ_1, θ_2 and θ_3. Figure 2 plots the 0.025, 0.5 and 0.975 pointwise sample quantiles from these 1000 conditional simulations. As expected it can be seen that the sample paths used to get the conditional events lay most of the time in the pointwise confidence intervals. In addition we can see that the sample quantile paths inherit the regularity driven by the shape parameter κ of the powered exponential correlation function and that there is less variability in regions close to some conditioning locations. Contrary to the results of Dombry et al. [2011] for Brown–Resnick processes, the sample quantiles do not converge to that of a unit Gumbel distribution since the Schlather process is not ergodic and cannot reach independence as we go far away from any conditioning location.

Since the conditional process $Z \mid Z(\mathbf{x}) = \mathbf{z}$ is not max-stable [Dombry et al., 2011], one need to integrate out with respect to the conditional event to retrieve the max-stability property. To this aim we generate 1000 independent conditional events $Z(\mathbf{x}) = \mathbf{z}$, $\mathbf{x}$ being fixed, and for each single conditional event one conditional realization of a Schlather process. Figure 3 compares the pairwise extremal coefficient estimates using the F-madogram [Cooley et al., 2006] to the theoretical extremal coefficient functions $\theta_1, \theta_2, \theta_3$ with $k = 5, 10, 15$ conditioning locations. As expected, whatever the number of conditioning locations and the spatial dependence structures are, the (binned) pairwise estimates match the theoretical curves indicating that our conditional simulations have the right spatial dependence structure.

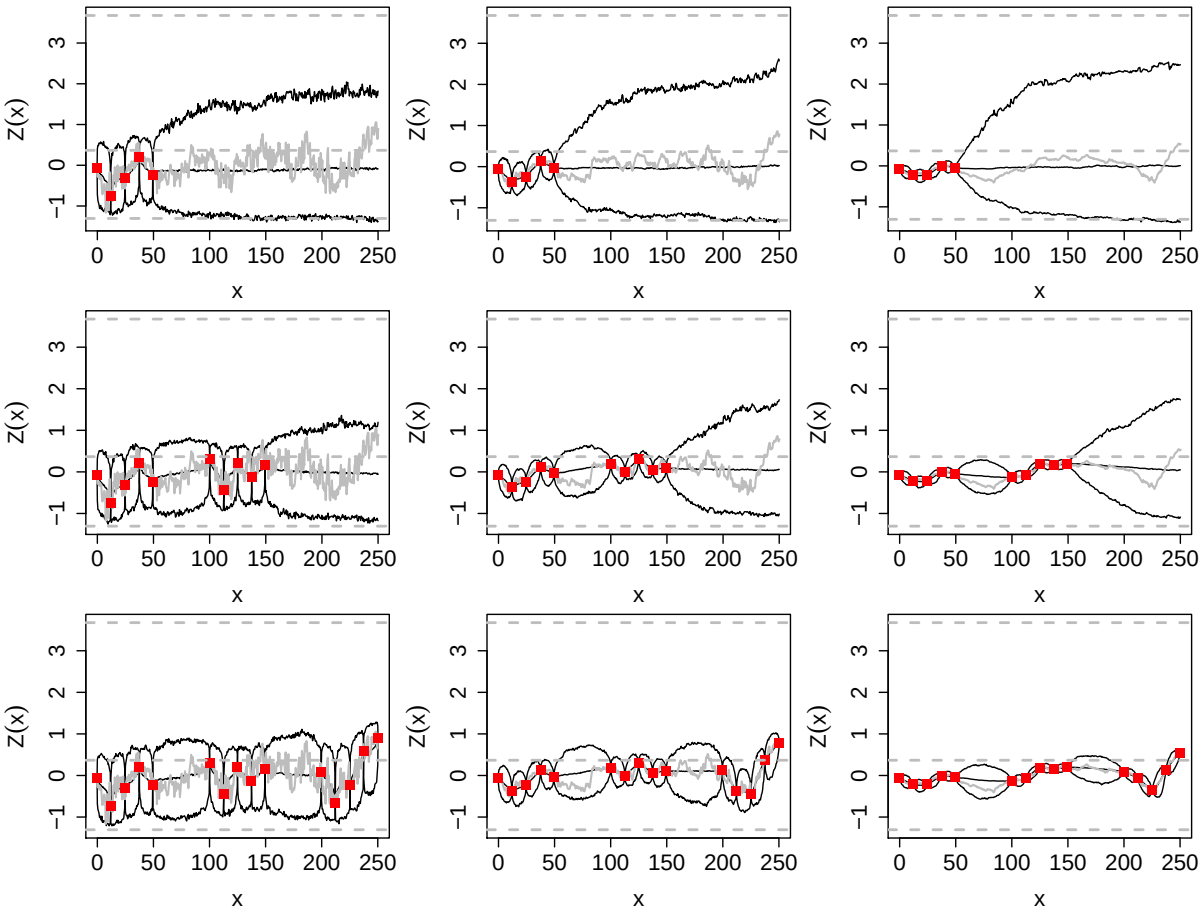

Figure 2: *Pointwise sample quantiles estimated from 1000 conditional simulations of Schlather processes with standard Gumbel margins and extremal coefficient function θ_1, θ_2 and θ_2 (left to right) and with $k = 5, 10, 15$ conditioning locations—top to bottom. The solid black lines show the pointwise 0.025, 0.5, 0.975 sample quantiles and the dashed grey lines that of a standard Gumbel distribution. The squares show the conditional points $\{(x_i, z_i)\}_{i=1,\ldots,k}$ and the solid grey lines correspond to the simulated paths of Figure 1.*

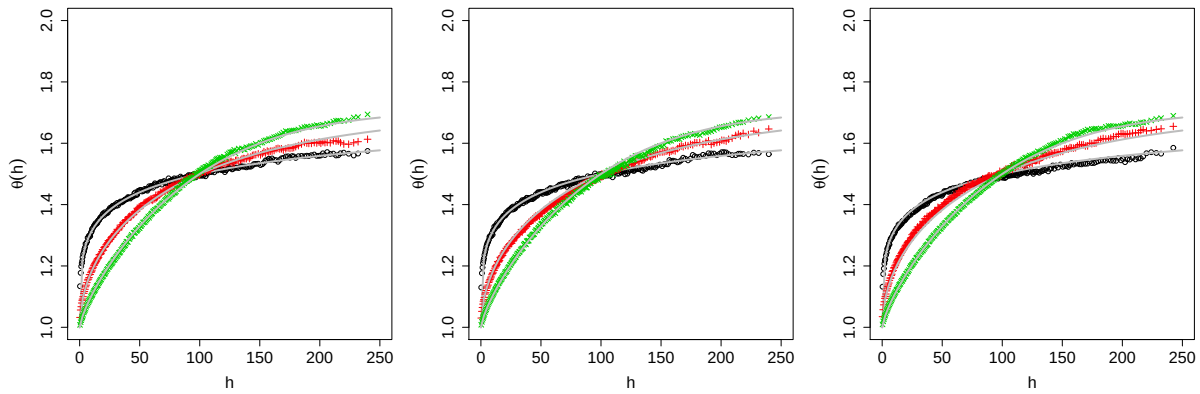

Figure 3: *Comparison of the pairwise extremal coefficient estimates (using a binned F-madogram with 250 bins on 1000 independent conditional simulations) and the theoretical extremal coefficient functions with $k = 5, 10$ and 15 conditioning locations—from left to right. The 'o', '+' and 'x' symbols correspond respectively to the spatial dependence configurations θ_1, θ_2 and θ_3. The solid grey lines correspond to the theoretical extremal coefficient functions.*

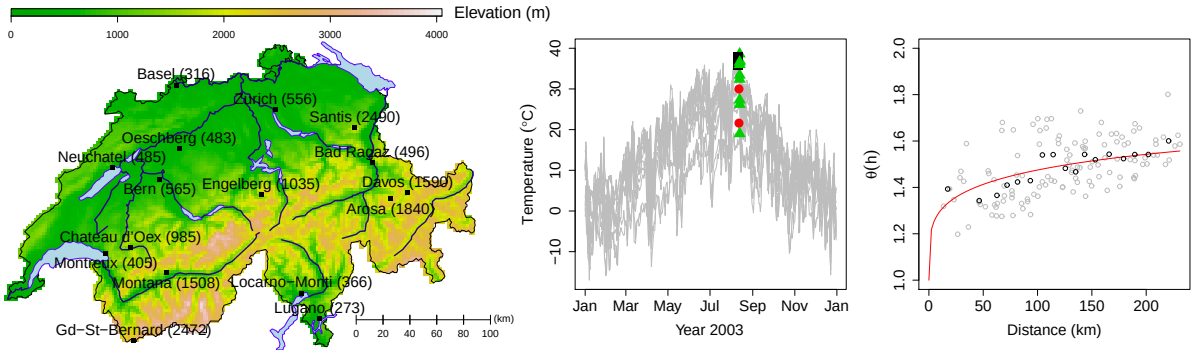

Figure 4: *Left: Topographical map of Switzerland showing the sites and altitudes in metres above sea level of 16 weather stations for which annual maxima temperature data are available. Middle: Times series of the daily maxima temperatures at the 16 weather stations for year 2003. The black squares, red circles and green triangles indicate the annual maxima that occurred respectively the 11th, 12th and 13th of August. Right: Comparison between the fitted extremal coefficient function from a Schlather process (solid red line) and the pairwise extremal coefficient estimates (gray circles). The black circles denote binned estimates with 16 bins.*

Table 2: *Empirical distribution of the partition size for the temperature data estimated from 10 parallel Markov chains of length 1000.*

Partition size	1	2	3	4	5–16
Empirical probabilities (%)	2.47	21.55	64.63	10.74	0.61

4 Application

In this section we apply our results to get conditional simulations of extreme temperatures. The data considered here were previously analyzed by Davison and Gholamrezaee [2011] and consist in annual maximum temperatures recorded at 16 sites in Switzerland during the period 1961–2005—see Figure 4.

Following the work of Davison and Gholamrezaee [2011], we consider a Schlather process with an isotropic powered exponential correlation function. Due to the lack of covariates others than longitude, latitude and elevation, we consider the following trend surfaces for the generalized extreme value distribution parameters

$$\mu(x) = \beta_{0,\mu} + \beta_{1,\mu}\mathrm{alt}(x), \tag{3}$$
$$\sigma(x) = \beta_{0,\sigma}, \tag{4}$$
$$\xi(x) = \beta_{0,\xi} + \beta_{1,\xi}\mathrm{alt}(x), \tag{5}$$

where $\mathrm{alt}(x)$ denotes the altitude above mean sea level (in kilometres) and $\{\mu(x), \sigma(x), \xi(x)\}$ are the location, scale and shape parameters of the generalized extreme value distribution at location x.

A preliminary study showed that the simultaneous fit of the marginal and dependence parameters induced a bias in the estimation of the spatial dependence structure probably owing to the use of too simple trend surfaces and we decided to fit separately the marginal parameters $\beta_{\cdot,\cdot}$ and the spatial dependence parameters λ, κ—the latter were estimated by maximizing the pairwise likelihood obtained by transforming the data to unit Fréchet margins using the empirical distribution function. The spatial dependence parameter estimates are $\hat{\lambda} = 260$ (149) and $\hat{\kappa} = 0.52$ (0.12) and the corresponding fitted extremal coefficient function, which is similar to some extent to our test case θ_3 in Section 3, is shown in the right panel of Figure 4.

In year 2003, western Europe was hit by a severe heat wave believed to be the hottest one ever recorded since at most 1540 ("2003 European heat wave", Wikipedia: The Free Encyclopedia). Switzerland was also largely impacted by this severe extreme event since the nation wide record temperature of 41.5°C was recorded that year in Grono, Graubunden—near Lugano. Consequently for our analysis we use as the conditional event the maxima temperatures observed in summer 2003—see Figure 4. Based on our fitted max-stable model and using the Gibbs sampler of Dombry et al. [2011], we simulate 10 parallel

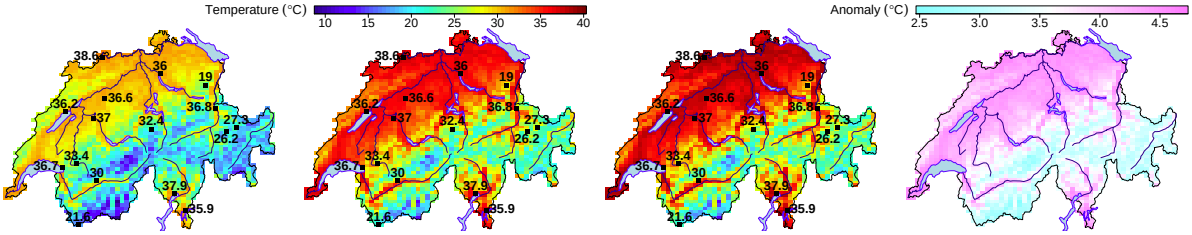

Figure 5: *From left to right: maps on a* 64×64 *grid of the pointwise* $0.025, 0.5$ *and* 0.975 *sample quantiles for temperature* (°C) *obtained from 10000 conditional simulations of a Schlather process. The squares show the conditional locations and the conditional values. The right panel shows the temperatures anomalies, i.e., the difference between the pointwise conditional medians and the pointwise unconditional medians estimated from the fitted trend surfaces* (3)–(5).

Markov chains of effective length 1000—with a burn-in period of length 500 and a thinning lag of 100 iterations. The empirical distribution of the partition size estimated from these Markov chains is shown in Table 2. We can see that around 90% of the time the conditional realizations were a consequence of at most three extremal functions. Since our original observations were not summer maxima but maximum daily values, a close inspection of the times series in year 2003 reveals that the hottest temperatures occurred between the 11th and 13th of August, see Figure 4, and, to some extent, corroborates the empirical distribution of Table 2.

Figure 5 shows the $0.025, 0.5$ and 0.975 pointwise sample quantiles obtained from 10000 conditional simulations on a 64×64 grid. The conditional pointwise median provides an estimation of the temperature at a given location while the 0.025 and 0.975 pointwise sample quantiles provide 95% pointwise confidence intervals. As expected, we can see that the largest temperatures occurred in the plateau region of Switzerland while temperatures were appreciably cooler in the Alps. The right panel of Figure 5 shows the difference between the pointwise conditional medians and the unconditional pointwise medians estimated from our fitted trend surfaces (3)–(5). The differences range between 2.5°C and 4.75°C and, as expected, the largest differences occur in the plateau region of Switzerland.

5 Conclusion

In this paper we derived the (regular) conditional distribution of the Schlather process and adapt the algorithm introduced by Dombry et al. [2011] to get conditional realizations from this process. The proposed framework was tested on simulated data and an application on extreme temperatures in Switzerland was given. Results show that our procedure gives accurate simulations. This work completes the one started by Dombry and Éyi-Minko [2011] and Dombry et al. [2011] and therefore enables the use of conditional simulations from widely used max-stable models. Future works could focus on the random set version of the Schlather process [Schlather, 2002] as well as the Smith model [Smith, 1990]. Although the (regular) conditional distribution of the former could be found following the lines of this paper, trying to get closed forms for the latter is likely to be more challenging since the spectral measure of the Smith process is not regular. The algorithms used for this work have been implemented in `C` within the `R` framework [R Development Core Team, 2011] and will be collected in the `R` package `SpatialExtremes` [Ribatet, 2011].

Acknowledgements

M. Ribatet was partly funded by the MIRACCLE-GICC and McSim ANR projects. The authors kindly acknowledge Prof. A. C. Davison and Dr. M. Gholam-Rezzaee for providing the Swiss temperature data set.

A Disintegration of $\Lambda_{\mathbf{x}}(A)$

In this appendix we show that the intensity measure of the Poisson point process $\{\varphi_i(\mathbf{x})\}_{i\geq 1}$ defined on $\mathbb{R}^k$ is absolutely continuous with respect to the Lebesgue measure and give closed form for its density.

It is straightforward to see that for all $\mathbf{x} \in \mathcal{X}^k$ and Borel set $A \subset \mathbb{R}^k$

$$\Lambda_{\mathbf{x}}(A) = \int_0^\infty \Pr[\sqrt{2\pi}\zeta\varepsilon(\mathbf{x}) \in A]\zeta^{-2}\mathrm{d}\zeta = \int_0^\infty \int_{\mathbb{R}^k} 1_{\left\{\sqrt{2\pi}\zeta\mathbf{y}\in A\right\}} f_{\mathbf{x}}(\mathbf{y})\mathrm{d}\mathbf{y}\zeta^{-2}\mathrm{d}\zeta,$$

where $f_{\mathbf{x}}$ denotes the density of the random vector $\varepsilon(\mathbf{x})$, i.e., a centered Gaussian random vector with covariance matrix $\Sigma_{\mathbf{x}}$. Now the change of variable $\mathbf{z} = \sqrt{2\pi}\zeta\mathbf{y}$ gives

$$\begin{aligned}
\Lambda_{\mathbf{x}}(A) &= (2\pi)^{-k/2} \int_0^\infty \int_A f_{\mathbf{x}}\left(\frac{\mathbf{z}}{\sqrt{2\pi}\zeta}\right) \zeta^{-(k+2)}\mathrm{d}\mathbf{z}\mathrm{d}\zeta \\
&= (2\pi)^{-k}|\Sigma_{\mathbf{x}}|^{-1/2} \int_0^\infty \int_A \exp\left(-\frac{1}{4\pi\zeta^2}\mathbf{z}^T\Sigma_{\mathbf{x}}^{-1}\mathbf{z}\right) \zeta^{-(k+2)}\mathrm{d}\mathbf{z}\mathrm{d}\zeta \\
&= (2\pi)^{-k}|\Sigma_{\mathbf{x}}|^{-1/2} \int_A \int_0^\infty \exp\left(-\frac{\zeta^2}{4\pi}\mathbf{z}^T\Sigma_{\mathbf{x}}^{-1}\mathbf{z}\right) \zeta^{k}\mathrm{d}\zeta\mathrm{d}\mathbf{z} \\
&= (2\pi)^{-k}|\Sigma_{\mathbf{x}}|^{-1/2} \int_A \frac{2\pi}{\mathbf{z}^T\Sigma_{\mathbf{x}}^{-1}\mathbf{z}} \mathbb{E}[X^{k-1}]\mathrm{d}\mathbf{z}, \qquad X \sim \text{Weibull}\left(\sqrt{\frac{4\pi}{\mathbf{z}^T\Sigma_{\mathbf{x}}^{-1}\mathbf{z}}}, 2\right) \\
&= (2\pi)^{-k}|\Sigma_{\mathbf{x}}|^{-1/2} \int_A \frac{2\pi}{\mathbf{z}^T\Sigma_{\mathbf{x}}^{-1}\mathbf{z}} \left(\frac{4\pi}{\mathbf{z}^T\Sigma_{\mathbf{x}}^{-1}\mathbf{z}}\right)^{(k-1)/2} \Gamma\left(\frac{k+1}{2}\right) \mathrm{d}\mathbf{z} \\
&= \int_A \lambda_{\mathbf{x}}(\mathbf{z})\mathrm{d}\mathbf{z},
\end{aligned}$$

where $\lambda_{\mathbf{x}}(\mathbf{z}) = \pi^{-(k-1)/2}|\Sigma_{\mathbf{x}}|^{-1/2}a_{\mathbf{x}}(\mathbf{z})^{-(k+1)/2}\Gamma\left\{(k+1)/2\right\}$ and $a_{\mathbf{x}}(\mathbf{z}) = \mathbf{z}^T\Sigma_{\mathbf{x}}^{-1}\mathbf{z}$.

References

Chilès, J.-P. and Delfiner, P. (1999). *Geostatistics: Modelling Spatial Uncertainty*. Wiley, New York.

Cooley, D., Naveau, P., and Poncet, P. (2006). Variograms for spatial max-stable random fields. In *Dependence in Probability and Statistics*, volume 187 of *Lecture Notes in Statistics*, pages 373–390. Springer, New York.

Davis, R. and Resnick, S. (1989). Basic properties and prediction of max-arma processes. *Advances in Applied Probability*, 21(4):781–803.

Davis, R. and Resnick, S. (1993). Prediction of stationary max-stable processes. *Annals Of Applied Probability*, 3(2):497–525.

Davison, A., Padoan, S., and Ribatet, M. (2011). Statistical modelling of spatial extremes. *To appear in Statistical Science*.

Davison, A. C. and Gholamrezaee, M. M. (2011). Geostatistics of extremes. *Proceedings of the Royal Society A: Mathematical, Physical and Engineering Science*.

Dombry, C. and Éyi-Minko, F. (2011). Regular conditional distributions of max infinitely divisible processes. *Submitted*.

Dombry, C., Éyi-Minko, F., and Ribatet, M. (2011). Conditional simulation of Brown–Resnick processes. *Submitted*.

Kabluchko, Z. and Schlather, M. (2010). Ergodic properties of max-infinitely divisible processes. *Stochastic Processes and their Applications*, 120(3):281–295.

Naveau, P., Guillou, A., and Cooley, D. (2009). Modelling pairwise dependence of maxima in space. *Biometrika*, 96(1):1–17.

Padoan, S., Ribatet, M., and Sisson, S. (2010). Likelihood-based inference for max-stable processes. *Journal of the American Statistical Association (Theory & Methods)*, 105(489):263–277.

R Development Core Team (2011). *R: A Language and Environment for Statistical Computing*. R Foundation for Statistical Computing, Vienna, Austria. ISBN 3-900051-07-0.

Ribatet, M. (2011). *SpatialExtremes: Modelling Spatial Extremes*. R package version 1.8-5.

Schlather, M. (2002). Models for stationary max-stable random fields. *Extremes*, 5(1):33–44.

Smith, R. L. (1990). Max-stable processes and spatial extreme. *Unpublished manuscript*.

Wang, Y. and Stoev, S. A. (2011). Conditional sampling for spectrally discrete max-stable random fields. *Advances in Applied Probability*, 443:461–483.

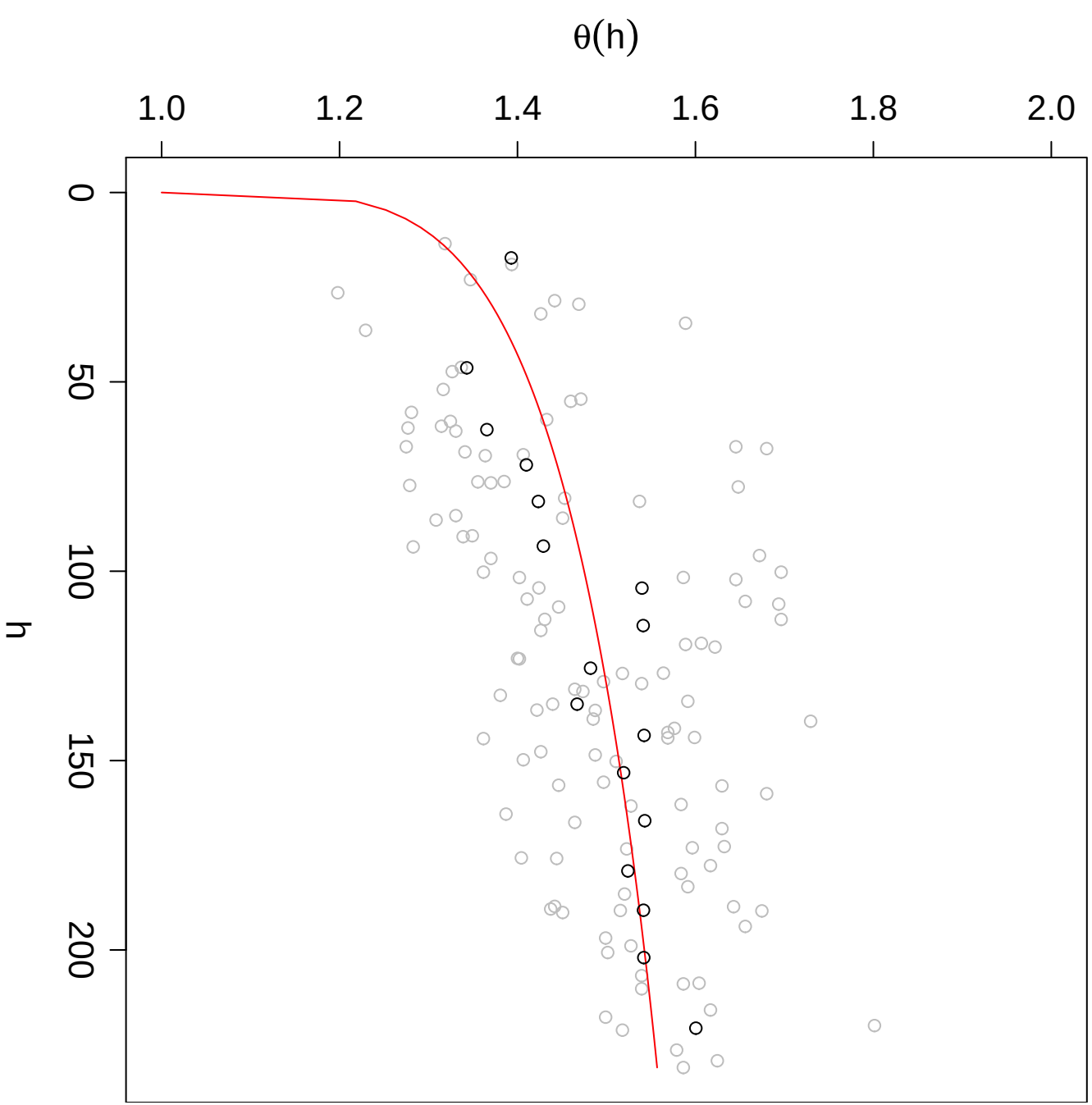
θ(h)
1.0
1.2
1.4
1.6
1.8
2.0
h
0
50
100
150
200